AD-A262 365

DTIC
ELECTE
MAR 1 7 1993
S C D

(2)

ARMY RESEARCH LABORATORY

Uniaxial Compressive Response of M26A1E1 as a Function of Temperature

George A. Gazonas
Michael G. Leadore

ARL-TR-79

February 1993

20000920309

NOTICES

REPORT DOCUMENTATION PAGE

Form Approved
OMB No. 0704-0188

1. AGENCY USE ONLY *(Leave blank)*

2. REPORT DATE
February 1993

3. REPORT TYPE AND DATES COVERED
Final, Feb 92 - May 92

4. TITLE AND SUBTITLE
Uniaxial Compressive Response of M26A1E1 as a Function of Temperature

5. FUNDING NUMBERS
1L162618AH80

6. AUTHOR(S)
George A. Gazonas and Michael G. Leadore

7. PERFORMING ORGANIZATION NAME(S) AND ADDRESS(ES)

8. PERFORMING ORGANIZATION REPORT NUMBER

9. SPONSORING/MONITORING AGENCY NAMES(S) AND ADDRESS(ES)
US Army Research Laboratory
ATTN: AMSRL-OP-CI-B (Tech Lib)
Aberdeen Proving Ground, MD 21005-5066

10. SPONSORING/MONITORING AGENCY REPORT NUMBER
ARL-TR-79

11. SUPPLEMENTARY NOTES

12a. DISTRIBUTION/AVAILABILITY STATEMENT
Approved for Public Release - Distribution is Unlimited

12b. DISTRIBUTION CODE

13. ABSTRACT *(Maximum 200 words)*

A joint Hercules-Olin M14 Replacement Program for the M865 round considered M26A1E1 gun propellant as a candidate replacement for the current M14 gun propellant. This report outlines the results of uniaxial compression tests on M26A1E1 propellant as a function of temperature, -40, -20, 20 and 50 degrees Celsius and constant strain rate, 100 sec 1/s. The mechanical behavior of M26A1E1 is quantified using various mechanical response parameters such as yield stress, yield strain, compressive modulus, "failure" modulus, and absorbed energy density. In general, the mechanical behavior of M26A1E1 is more sensitive to temperature than M14. However, M26A1E1 is less susceptible to fracture damage than M14 over the temperature range -40 to 50 degrees Celsius. Scanning electron microscopy (SEM) of "cold-fractured" surfaces of M26A1E1 reveal the presence of undissolved nitrocellulose (NC) fibers on the order of 20 -58 micrometers. Some NC fibers "pull-out" during the cold-fracture process and leave behind a depression in the propellant surface. The surface of the depression reacts with the electron beam at high magnification forming blisters and extensional cracks.

14. SUBJECT TERMS
Mechanical Properties, Propellants, Compressive Testing, M14, M26A1E1, Propellant Fracture

15. NUMBER OF PAGES
32

16. PRICE CODE

17. SECURITY CLASSIFICATION OF REPORT	18. SECURITY CLASSIFICATION OF THIS PAGE	19. SECURITY CLASSIFICATION OF ABSTRACT	20. LIMITATION OF ABSTRACT
UNCLASSIFIED	UNCLASSIFIED	UNCLASSIFIED	SAR

NSN 7540-01-280-5500

Standard Form 298 (Rev. 2-89)
Prescribed by ANSI Std. 239-18 298-102

INTENTIONALLY LEFT BLANK.

TABLE OF CONTENTS

INTENTIONALLY LEFT BLANK.

LIST OF FIGURES

LIST OF TABLES

INTENTIONALLY LEFT BLANK.

ACKNOWLEDGMENT

We wish to thank Mr. Christopher Gillich for performing SEM observations and preparing the propellant morphology report and Dr. Robert Lieb for assistance in interpreting the SEM propellant morphology micrographs.

INTENTIONALLY LEFT BLANK.

1. INTRODUCTION

The Fracture Mechanics Team (FMT) at the BRL became involved in a joint Hercules-Olin M14 Replacement Program whose objectives were to find a propellant replacement for the M865 round. The proposed replacement propellant, M26A1E1 (Hercules experimental formulation, HES-9520.25), is a modification of the M14 propellant. Some advantages of the M26A1E1 propellant include, 1) low production cost, 2) low propellant hygroscopicity, 3) elimination of the carcinogen, dinitrotoluene, (DNT) from the M14 formulation, 4) successful use with the 152-mm Sheridan tank round, and 5) the production process is easily transferred to other propellant facilities.

This report outlines the results of uniaxial compression testing of M26A1E1 propellant as a function of temperature, -40, -20, 20, and 50 degrees Celsius and constant strain rate, 100 sec^{-1}. Of particular interest is whether fractures develop in the propellant as a result of uniaxial deformation, since the presence of fracture damage has been linked to both the vulnerability response (Lu et al. 1991) and enhanced apparent burning rate (Gazonas, Juhasz and Ford 1991) in propellants.

A comparison of the mechanical response parameters (e.g. yield stress and strain, compressive and failure moduli, absorbed energy density) of M14 and M26A1E1 as a function of temperature are also provided. Photographs of the deformed propellant are included as an aid in the description of the macroscopic deformation mechanisms and scanning electron micrographs (SEM) provide a morphological description of the undeformed propellant.

2. EXPERIMENTAL PROCEDURE

2.1 Specimen Preparation. The seven-perforation granular propellant (25 grams) was shipped from the Hercules, Inc., Kenvil, New Jersey facility in an explosion-proof cylinder. The

granular propellant starting material (M26A1E1 lot # HES-9520.25) was cut into right-circular cylinders using an Isomet double-bladed saw. A double-bladed saw was used to simultaneously cut both specimen ends parallel to each other and to help maintain coaxial deformation with the cylinder axis. Specimen aspect ratio, length-to-diameter (l/d), is about 2/1. The inert lubricant, molybdenum disulfide, MoS_2, was applied sparingly to the specimen ends to reduce end friction effects and test variability (Gazonas and Ford 1992). The M14 specimens (lot # RAD-PD-066-1) were prepared and tested in the same fashion in an earlier study (Lu et al. 1991). Propellant chemical compositions appear in Table 1.

Table 1. Chemical Compositions of M14 and M26A1E1 Propellants

Composition (%)	M14[a]	M26A1E1[b]
NC (13.15%N)-Nitrocellulose	89.0	65.55
DNT-Dinitrotoluene	8.0	-
NG-Nitroglycerin	-	23.51
DBP-Dibutyl Pthalate	2.0	9.75
DPA-Diphenylacetate	1.0	-
EC-Ethyl Centralite	-	0.98
Carbon Black	-	0.21

[a]Lu et al. 1992

[b]Furrier 1992

2.2 Test Apparatus, Data Acquisition and Data Reduction. The High Rate 810 MTS material test system (Figure 1) consists of a conventional two-pole press with a servohydraulically actuated ram that operates from quasi-static velocities to a maximum velocity of about 12 meters/sec; the maximum velocity imparts a strain rate of 1200 sec^{-1} on a 10 millimeter long specimen. A Thermotron temperature controller, Model 5200, permits thermal conditioning of specimens from -85 to

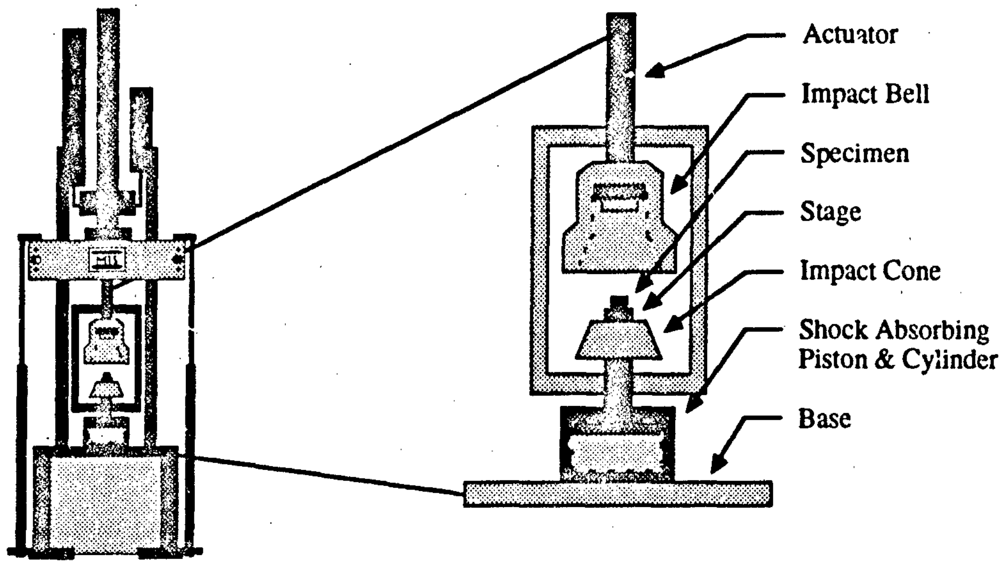

Figure 1. Servohydraulic Test Apparatus.

90 degrees Celsius in an air-circulating oven/refrigerator that houses both upper and lower pistons during testing. Specimens are uniformly heated/cooled and thermally conditioned at the test temperatures -40, -20, 20 and 50 degrees Celsius for at least 30 minutes before each test. Uniaxial compression tests are performed at a constant strain rate of 100 sec^{-1} by computer control of the piston velocity via feedback from an externally-mounted, linear-variable-differential-transformer (LVDT), MTS Model 244.11. Force is measured with a 60 kN, quartz-piezoelectric, force transducer, Kistler Type 9031A, that is mounted on the upper moving piston. Apparatus stiffness is measured at 91.87 ± 4.8 kN/mm (Gazonas 1991).

The raw force and displacement data are acquired, stored, and analyzed using an IQ-300 multichannel processing digital oscilloscope. The raw force and displacement data are reduced to engineering stress, σ, versus strain, ε, by normalizing measured quantities to initial specimen area and specimen length respectively. Force data are corrected for temperature changes since the force transducer and piston assembly are housed within the thermal conditioning chamber.

An automatic data reduction program was written for the IQ-300 processing oscilloscope in

an effort to reduce the arbitrariness and operator-dependent preferences involved with picking points from stress-strain curves. For example, in this study, the yield stress is defined as the stress level where the material most rapidly loses its ability to sustain load; the yield stress level is determined by finding the minimum in the second-derivative of stress with respect to time. The second-derivative stress versus time data are somewhat noisy because of the particular finite-difference algorithm employed for calculating derivatives of oscilloscope trace data. However, the derivative data are substantially improved by two successive data smoothings. Satisfactory results are obtained if the first derivative of stress is first smoothed with a twenty-point moving average and the second derivative of stress is then smoothed with a twenty-five-point moving average. Automation of stress-strain data analysis through software programming permits determination of unbiased, operator-independent estimates of mechanical properties.

Equally arbitrary definitions of the yield stress (Malvern 1969), such as the proportional limit definition (stress level at the end of the linear range) or offset method definition (stress level after 0.2 percent offset strain), were not viable as yield stress definitions, since for the former definition a suitable linear range is difficult to determine for these materials, and for the latter definition the yield would occur at fractions of a percent of maximum stress and the strain dependence of yield could not be investigated. Other mechanical response parameters include, the yield strain, energy density absorbed per unit undeformed volume, and compressive and "failure" moduli (see Figure 2

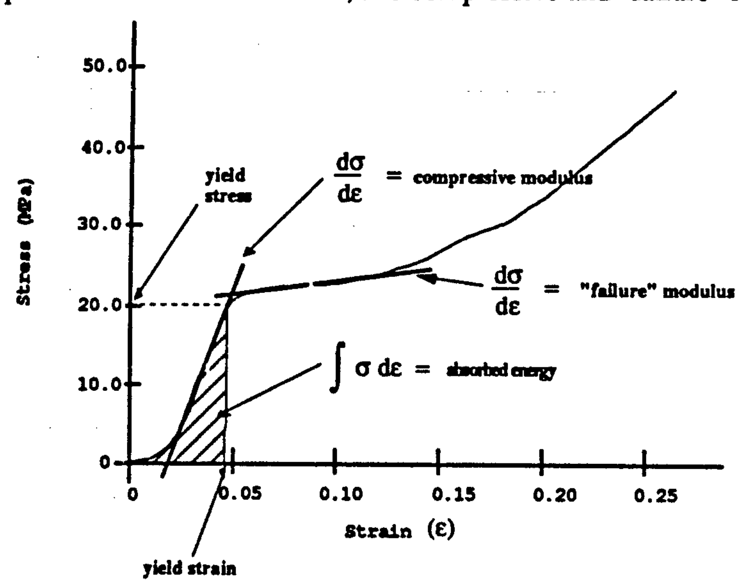

Figure 2. Definitions of Mechanical Response Parameters.

for a graphical illustration of the definition of these quantities).

After data reduction is completed, the mechanical property data and other pertinent test information are transferred to a Compaq 286 personal computer via an RS-232 communications port. The data are then imported into a DBASE III Plus database library for subsequent comparison and correlation. A total of 31 mechanical property fields are stored and include propellant ID, lot number, date, compressive moduli, stress and strain at yield, energy absorbed at fixed strain levels from 0.025 to 0.25, specimen dimensions, test temperature, strain rate and a character array for physical description of the deformed propellant.

3. UNDEFORMED STARTING MATERIAL: SEM MORPHOLOGY

The M26A1E1 propellant is longitudinally cold-fractured after the specimen is thermally conditioned in dry-ice for five minutes. The fracture surface is smooth with no observed cracks or voids (Figure 3a). Subsequent SEM micrographs (Figures 3b through 3j) are sequentially magnified for illustrative purposes. The specimen contains undissolved nitrocellulose fibers, not uncommon in highly nitrated nitrocellulose. The diameter of the nitrocellulose fibers range between 20-58 micrometers. Also observed are very small particles with diameters less then 2 micrometers (possibly carbon-black). Some nitrocellulose fibers appear to have been pulled out when the specimen was prepared by cold-fracturing. The pull-out regions appear as depressions or "footprints" of undissolved nitrocellulose fibers (Figures 3g and 3h). A blister of roughly circular shape which contains surface extensional cracks forms when the electron beam is focussed over the area of the "footprint" (Figure 3j). The area immediately adjacent to the depression shows less reactivity to the electron beam. The inhomogeneous reaction sensitivity of the propellant surface might be explained by, 1) a higher concentration of energetic material (possibly nitroglycerin) in the depression or 2) surface roughness or topographic differences between the depression and adjacent areas. The high degree of surface reactivity is unusual for double-base propellants and further research is needed to fully understand the phenomenon.

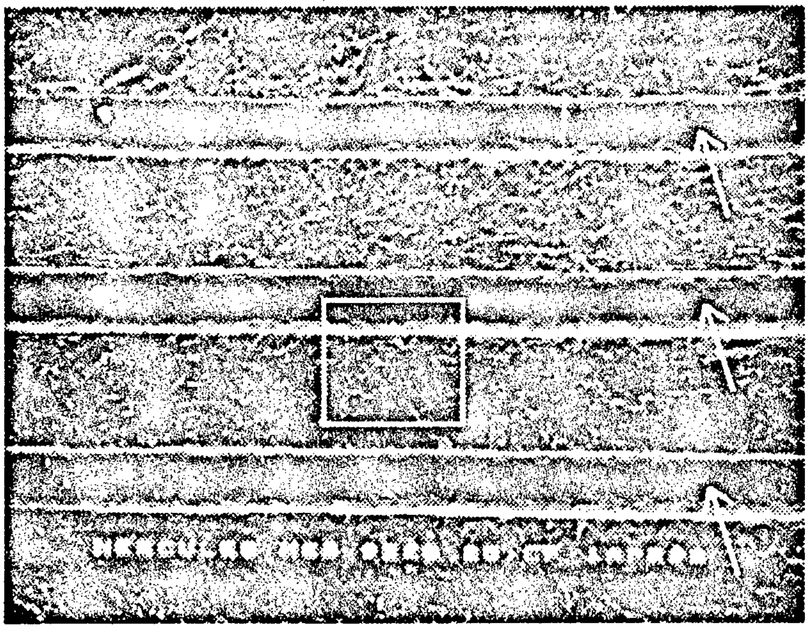

a) Longitudinal section showing cross-section through three perforations (100 μ = 1mm). Highlighted rectangle is magnified in subsequent photographs.

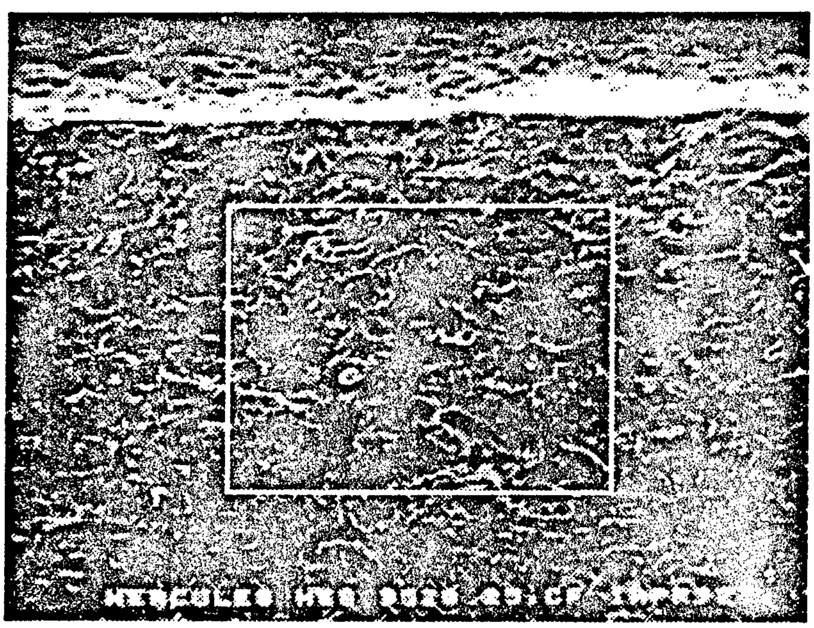

b) Enlarged section of Figure 3a) (100 μ = 5mm).

Figure 3. SEM micrograph of longitudinally "cold-fractured" propellant grain.

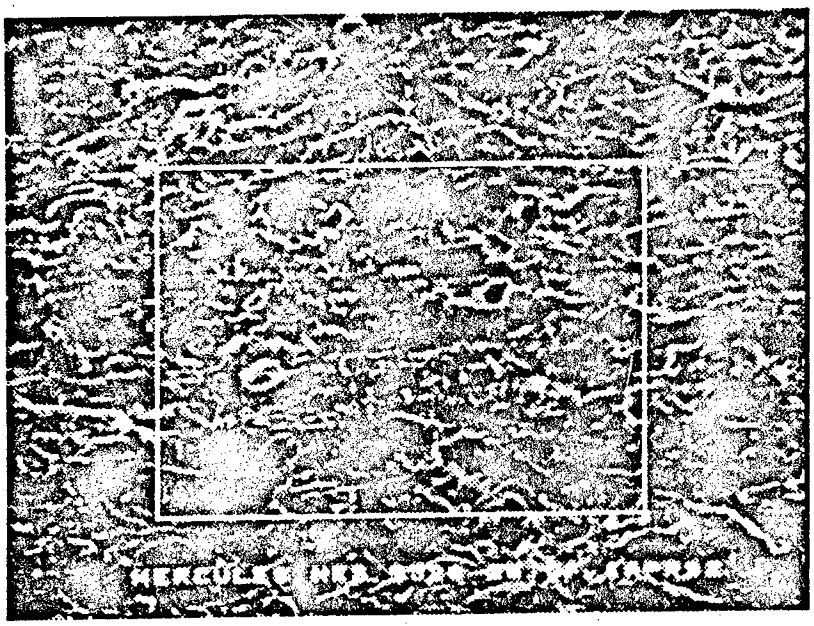

c) Enlarged section of Figure 3b) (100 μ = 10 mm).

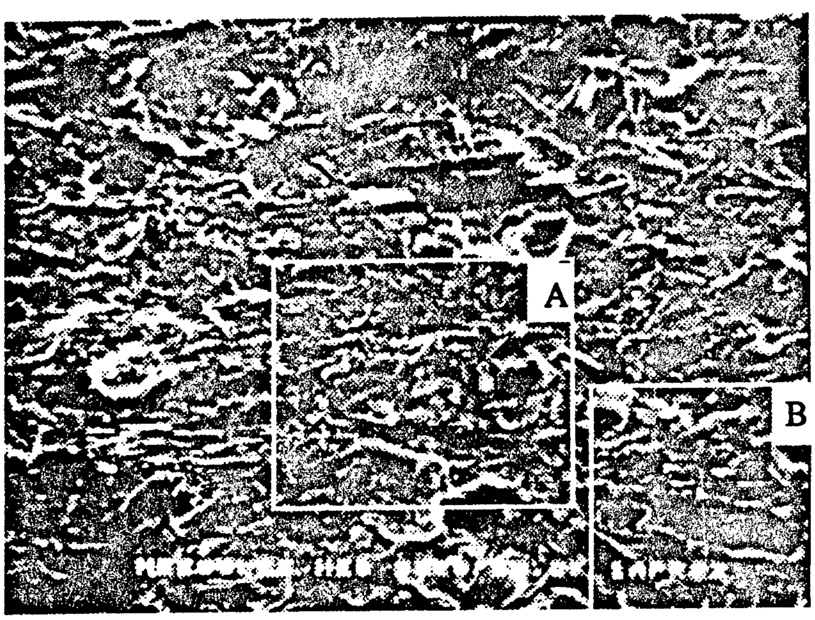

d) Enlarged section of Figure 3c) (10 μ = 2 mm).

Figure 3. <u>SEM micrograph of longitudinally "cold-fractured" propellant grain (cont'd)</u>

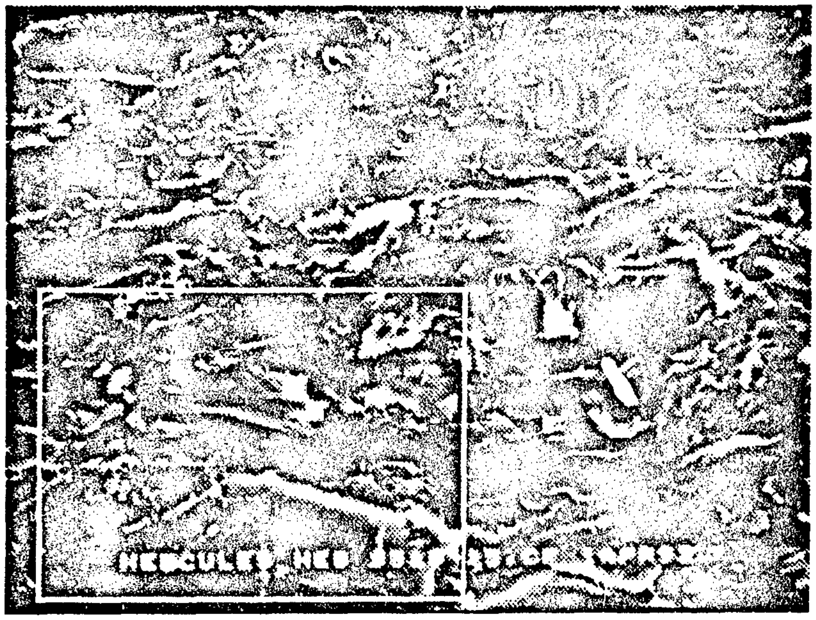

e) Enlarged section of Figure 3d-A) (10 μ = 5 mm).

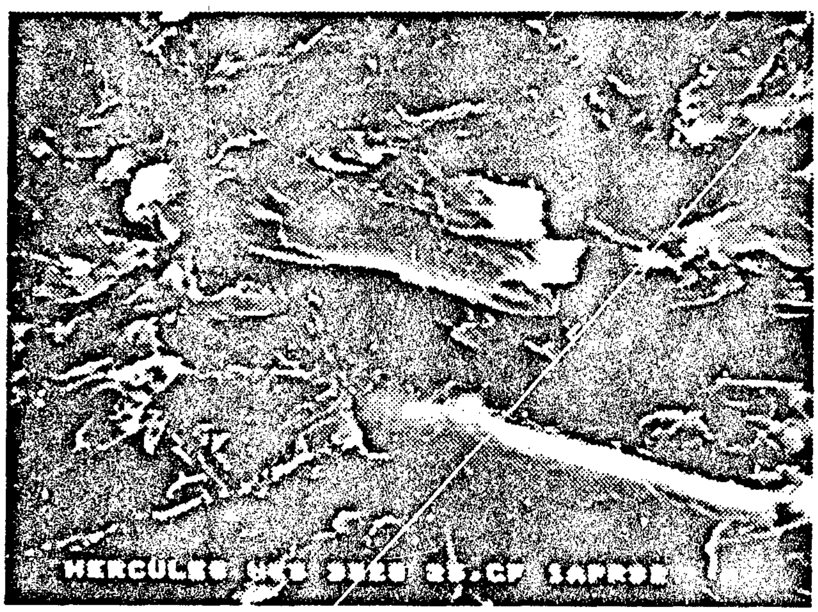

f) Enlarged section of Figure 3e) (10 μ = 10 mm).

Figure 3. SEM micrograph of longitudinally "cold-fractured" propellant grain (cont'd)

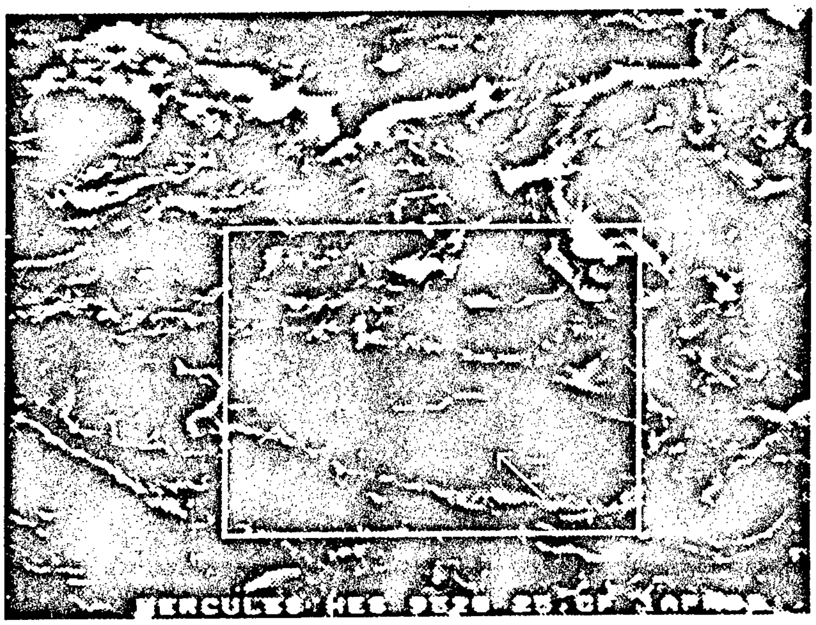

g) Enlarged section of Figure 3d-B) showing surface depression (10 μ = 5 mm).

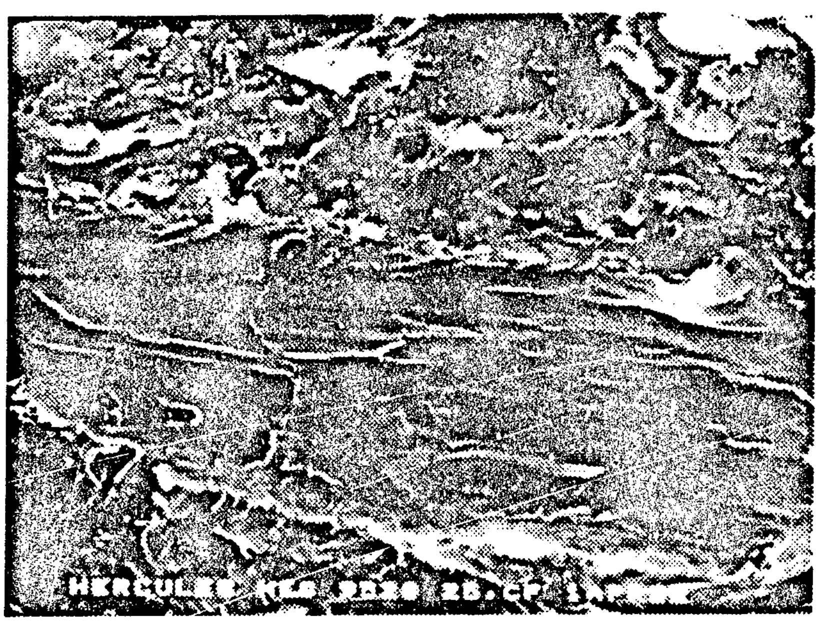

h) Enlarged section of Figure 3g) (10 μ = 10 mm).

Figure 3. <u>SEM micrograph of longitudinally "cold-fractured" propellant grain (cont'd)</u>

i) Circular blister with surface cracks in depression. The electron beam is focussed over the area in Figure 3j and is photographed at the magnification (10 μ = 10 mm) above.

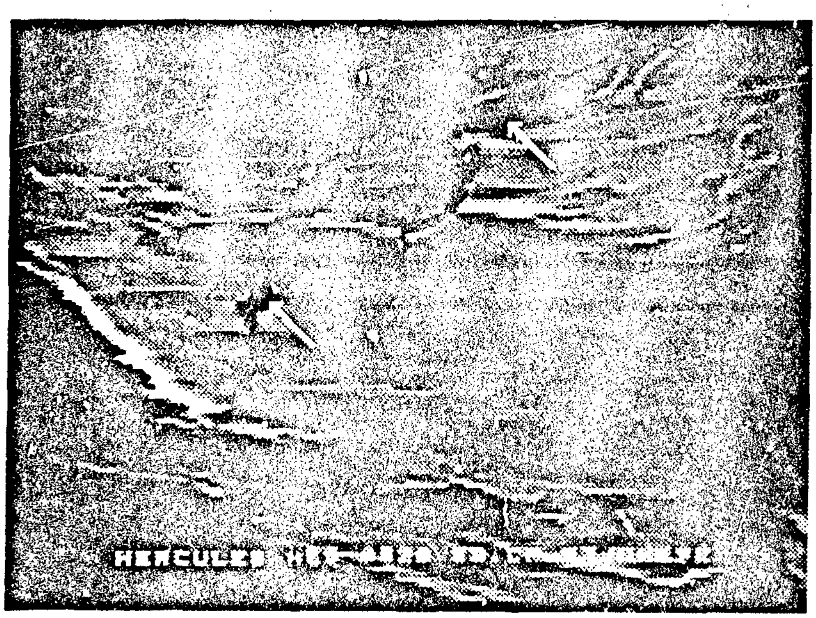

j) "Extensional" cracks in enlarged section of Figure 3i) (1 μ = 5 mm).

Figure 3. <u>SEM micrograph of longitudinally "cold-fractured" propellant grain (cont'd)</u>

4. UNIAXIAL COMPRESSION TEST RESULTS

Photographs of damaged M26A1E1 specimens at each test temperature, -40, -20, 20 and 50 degrees Celsius, appear in Figures 4a) through 4d) respectively. All specimens are uniaxially deformed at a strain rate of 100 sec^{-1} to a strain level of about 40 percent. Specimens deformed at -40 degrees Celsius fracture through axial splitting and fragment into two or more pieces (Figure 4a). Fracture is also observed in specimens deformed at -20 degrees Celsius, yet specimen fragmentation does not occur (Figure 4b). Some axial splitting is also observed in specimens deformed at 20 and 50 degrees Celsius (Figures 4c and 4d).

Summary plots (5 tests per curve) which illustrate the experimental results for the uniaxial compression of M26A1E1 and M14 at temperatures of -40, -20, 20 and 50 degrees Celsius and a strain rate of 100 sec^{-1} appear in Figures 5 and 6 respectively. Both propellants exhibit "softening" behavior as temperature increases. Thermal softening is common in materials with temperature-dependent deformation mechanisms. The time axes in these figures are readily converted to strain by multiplying by the strain rate, 100 sec^{-1}. The mechanical behavior of M26A1E1 is very similar to that of JA2 (Gazonas and Ford 1992), and exhibits continual workhardening behavior at all test temperatures except at -40 degrees Celsius where the material slightly worksoftens after reaching a maximum stress level (Figure 5). The macroscopic deformation response of M26A1E1 is ductile since the material maintains significant stress levels to strain levels of 40 percent. In contrast to M26A1E1, fragmentation, and a deterioration of the mechanical strength of M14 is observed at the colder test temperatures, -20 and -40 degrees Celsius (Figure 6).

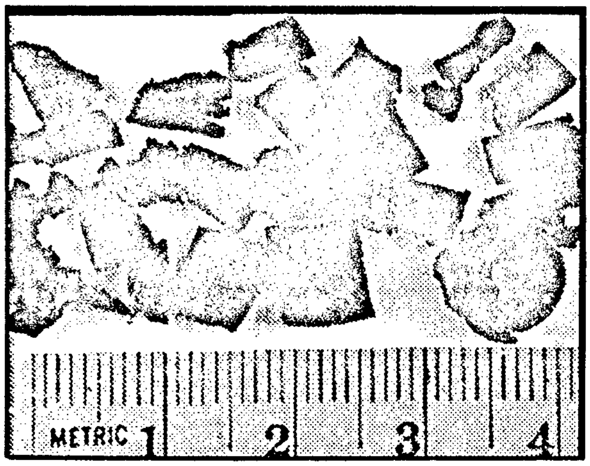

a) - 40 °C

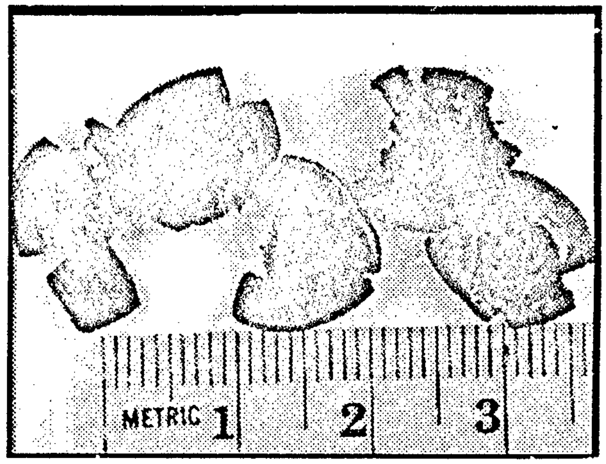

b) - 20 °C

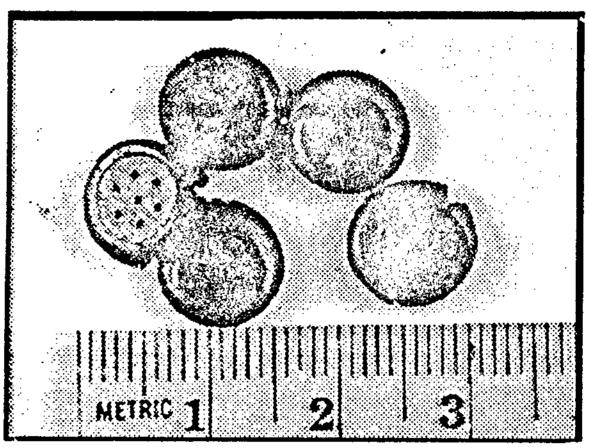

c) 20 °C

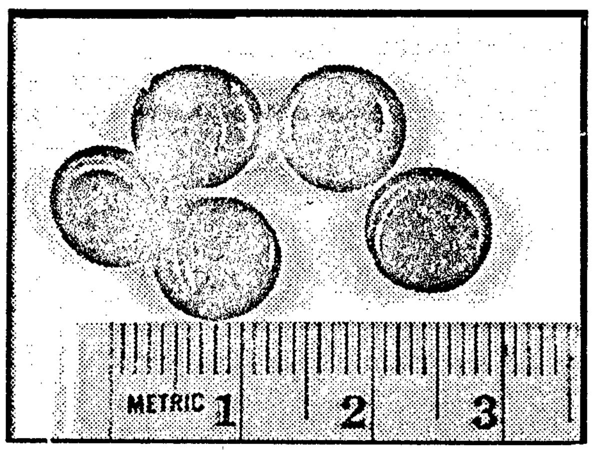

d) 50 °C

Figure 4. Photographs of M26A1E1 Propellant Uniaxially Damaged at Various Temperatures.

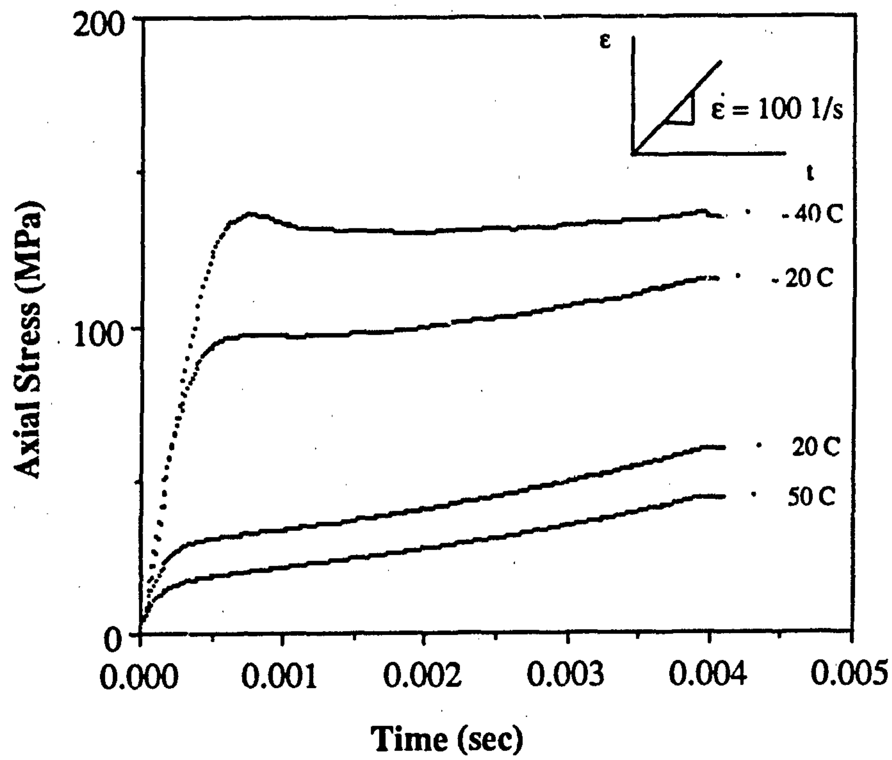

Figure 5. Axial Stress versus Time for Various Temperatures in M26A1E1 Propellant.

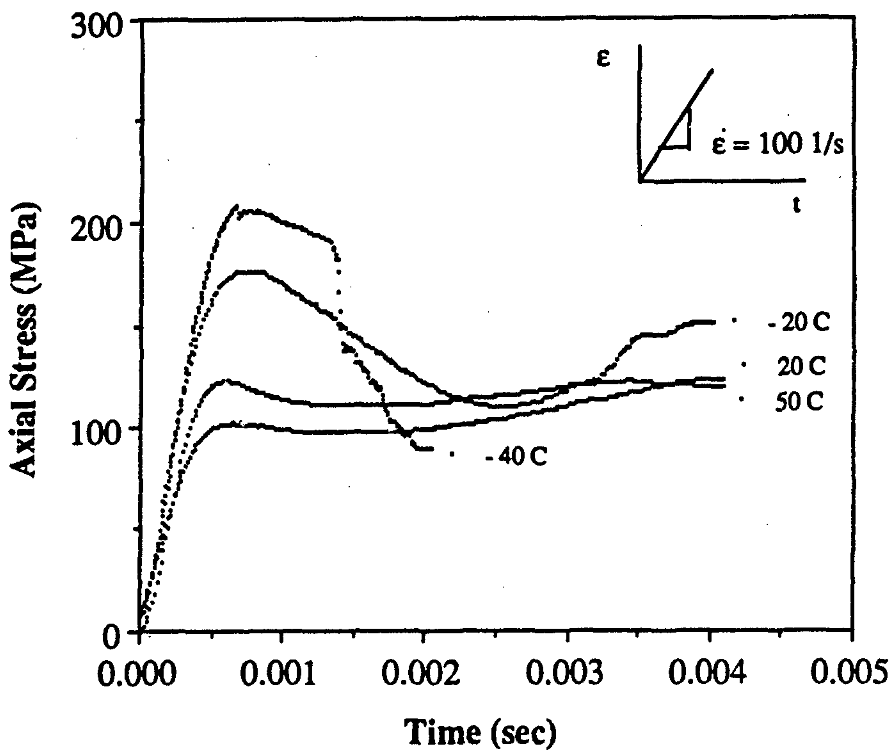

Figure 6. Axial Stress versus Time for Various Temperatures in M14 Propellant.

5. MECHANICAL RESPONSE PARAMETERS

Certain mechanical response parameters aid in quantifying the macroscopic deformation behavior of M26A1E1 and M14 propellants. These parameters were illustrated earlier (Figure 2), i.e., yield stress and strain, energy density absorbed per unit undeformed volume, and compressive and "failure" moduli, and appear as a function of temperature for M26A1E1 and M14 propellants in tabular form in Table 2.

Table 2. Comparitive Mechanical Properties of M26A1E1 and M14 Propellants as a Function of Temperature, (a) M26A1E1 (HES-9520.25), (b) M14 (RAD-PD-066-1). Standard deviations are estimated from 5 tests.

Temp., °C	Yield Stress, MPa	Yield Strain, %	Modulus, GPa	Failure Modulus, GPa	Energy Density/Unit Vol., MPa
			(a)		
-40	140.2 ± 5	5.5 ± 0.2	2.8 ± 0.2	-0.09 ± 0.01	31.5 ± 0.9
-20	89.5 ± 3	4.4 ± 0.2	2.05 ± 0.05	0.019 ± 0.002	22.6 ± 0.4
20	28.1 ± 1	2.7 ± 0.3	0.8 ± 0.1	0.057 ± 0.005	8.7 ± 0.3
50	16.6 ± 2	2.1 ± 0.2	0.51 ± 0.04	0.054 ± 0.003	5.6 ± 0.2
			(b)		
-40	196.4 ± 16	4.8 ± 0.2	4.2 ± 0.5	-0.5 ± 0.2	19.1 ± 4
-20	166.5 ± 7	4.4 ± 0.5	3.7 ± 0.3	-0.36 ± 0.02	19.4 ± 2
20	118.3 ± 7	4.4 ± 0.4	2.9 ± 0.3	-0.14 ± 0.01	25.4 ± 2
50	100.8 ± 7	4.1 ± 0.3	1.9 ± 0.2	-0.031 ± 0.006	22.4 ± 2

The mechanical response parameters are also plotted in Figures 7 through 11. Polynomial expressions are included in each figure for determination of mechanical responses at temperatures other than those provided in Table 2. The yield stress decreases as temperature increases in both M26A1E1 and M14 propellants, yet there is a divergence of the yield stress at higher temperatures indicating that thermally activated deformation mechanisms are more important in M26A1E1 (Figure 7). The yield strain is also observed to decrease as temperature increases in both propellants (Figure 8). In M26A1E1, the yield strain is reduced by nearly a factor of three whereas in M14 the yield strain is reduced by only a factor of 1.2 over the temperature range from -40 to 50 degrees Celsius. Yield strain insensitivity to strain rate and temperature was also observed in previous uniaxial deformation studies on M30 gun propellant (Gazonas and Ford 1992). The compressive modulus of M26A1E1 is also seen to be more sensitive to temperature changes than the compressive modulus of M14 (Figure 9). At 50 degrees Celsius, M14 is about 3.5 times "stiffer" than M26A1E1. The opposite behavior is observed in the post-failure regime, where M14 propellant rapidly loses the ability to sustain load at colder temperatures due to crack coalescence and fragmentation of the specimen (Figure 10). Finally, the absorbed energy density per unit undeformed volume (obtained by integrating the area under the stress-strain curve to a strain level of 0.25, see Figure 2) is also relatively insensitive to temperature in M14 (Figure 11). In M26A1E1, the decrease in the absorbed energy density with temperature is primarily due to the decrease in stress level sustainable in the propellant as temperature is increased (Figure 5).

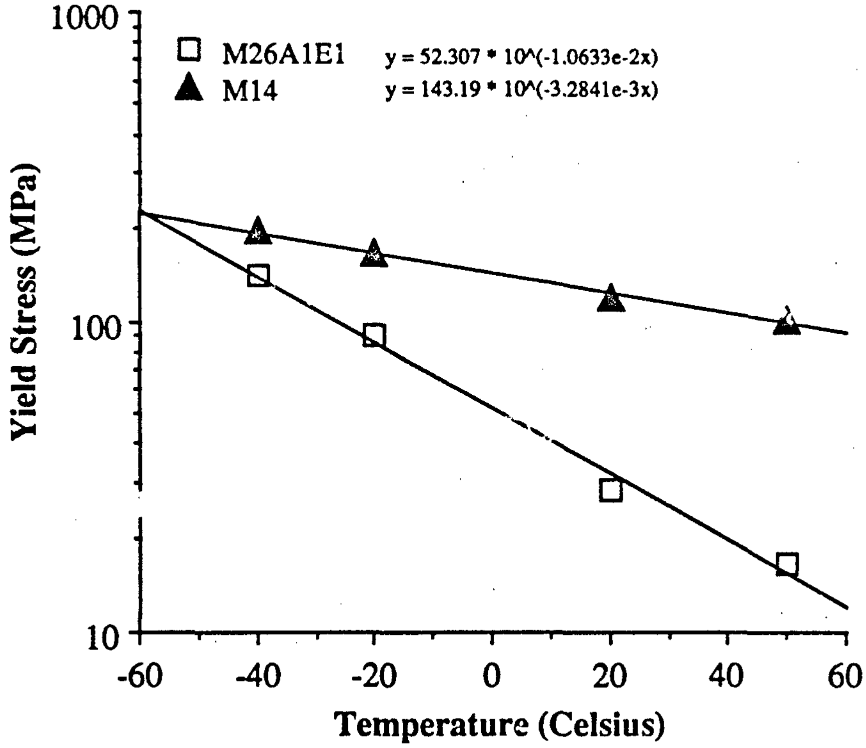

Figure 7. Yield Stress versus Temperature.

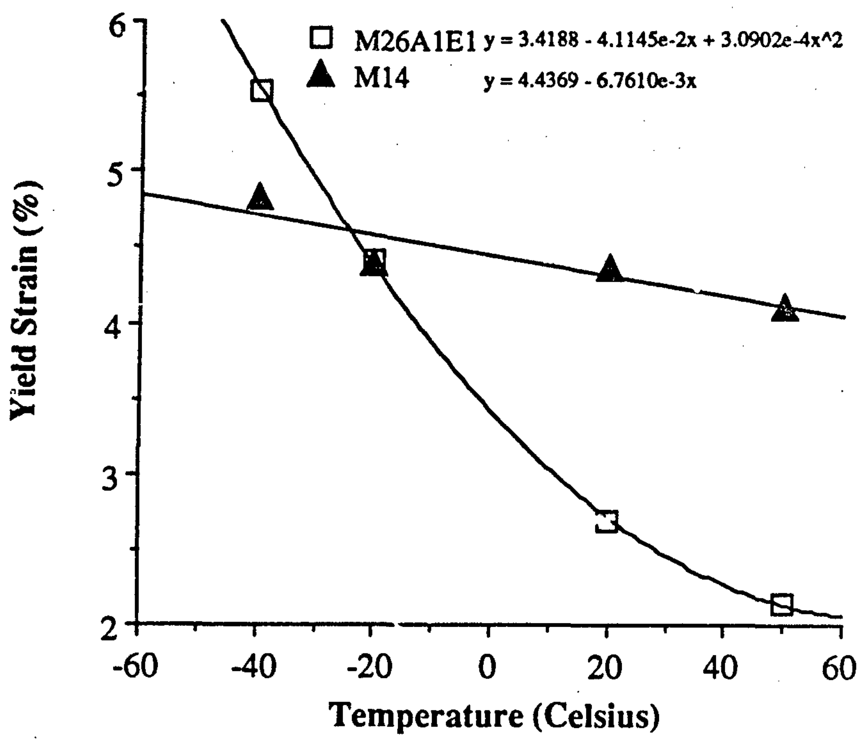

Figure 8. Yield Strain versus Temperature.

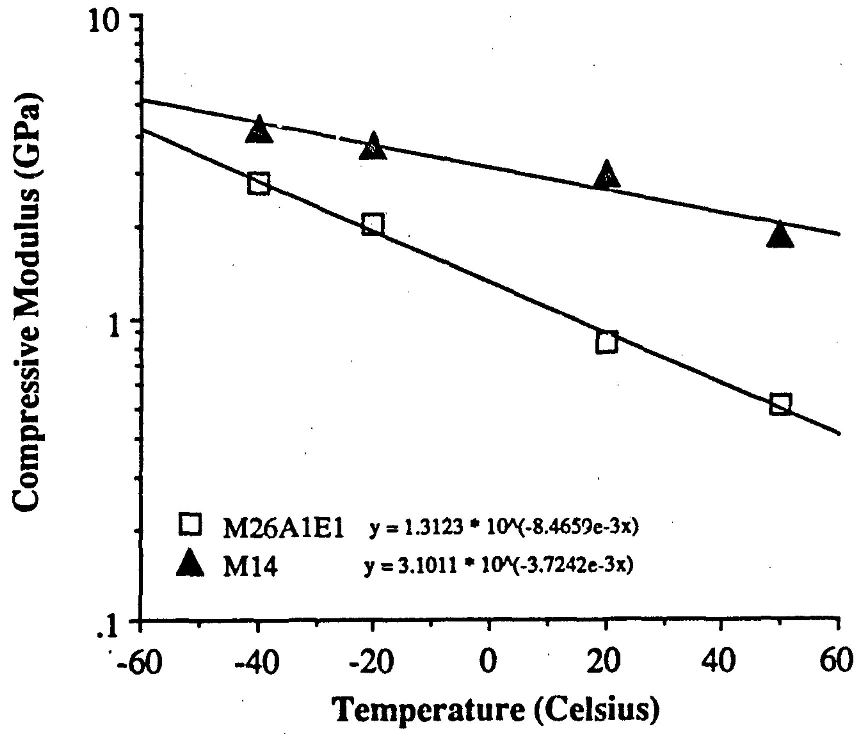

Figure 9. Compressive Modulus versus Temperature.

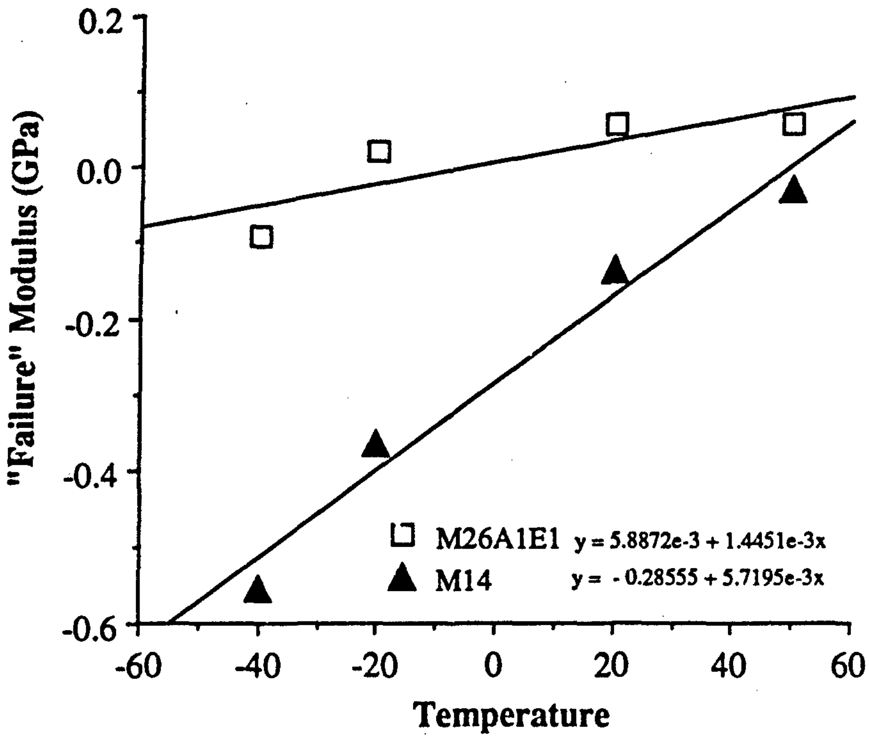

Figure 10. "Failure" Modulus versus Temperature.

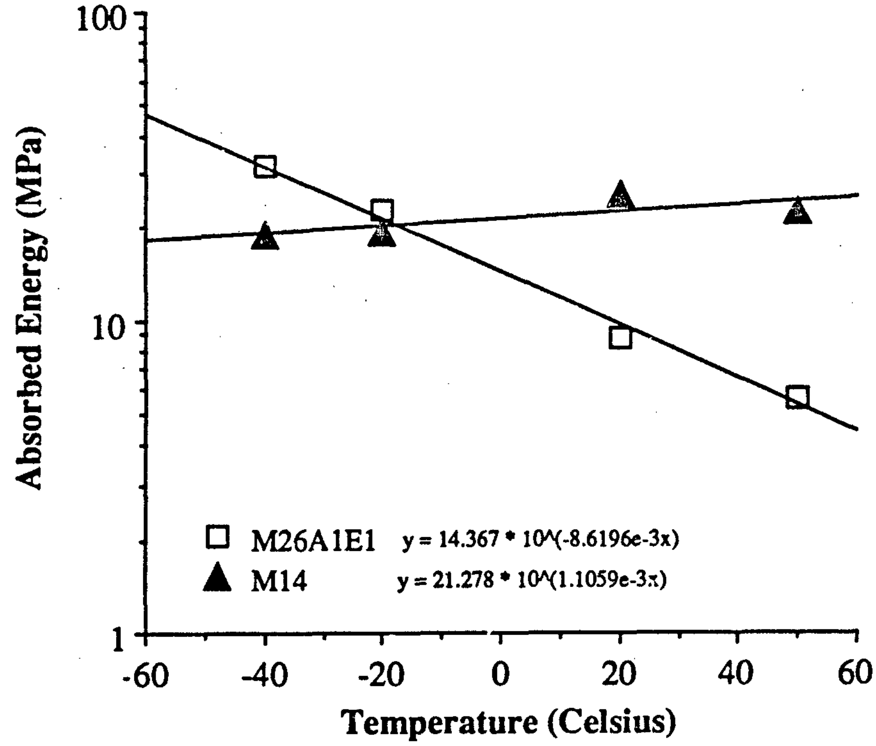

Figure 11. Absorbed Energy versus Temperature.

6. SUMMARY AND CONCLUSIONS

1) The uniaxial compressive response of M26A1E1 propellant is determined as a function of temperature, -40, -20, 20 and 50 degrees Celsius and constant strain rate, 100 sec^{-1}, and compared with the mechanical response of M14 propellant.

2) Axial splitting is observed in all M26A1E1 specimens deformed to 40 percent strain, but fragmentation into two or more pieces is only observed in those specimens tested at -40 degrees Celsius.

3) Scanning electron microscopy of longitudinally cold-fractured specimens of M26A1E1 reveals the presence of undissolved nitrocellulose fibers on the order of 20 - 58 micrometers. Depressions in the propellant surface form as a result of "pull-out" of the nitrocellulose fibers during the cold-fracture process. The depression areas are also highly reactive to the incident electron beam and surface decomposition by blistering occurs as the energy density of the electron beam is increased. Regions outside the depression show less reactivity and indicate that the depression surface might contain a higher concentration of energetic material (possibly nitroglycerin) than adjacent areas. It is also possible that surface roughness or topographic differences between the depression and adjacent areas cause the inhomogeneous surface reactivity. Further research is needed to study the phenomenon.

4) A comparison of the mechanical response parameters, yield stress and strain, compressive modulus, and absorbed energy density, between M26A1E1 and M14 propellants reveals that the mechanical response of M26A1E1 propellant is more sensitive to temperature than M14 propellant. However, the "failure" modulus in M14 propellant is more sensitive to temperature since fracture deformation mechanisms dominate in this material.

5) Since M26A1E1 propellant is less susceptible to fracture damage than M14 propellant over the temperature range -40 to 50 degrees Celsius and at a strain rate of 100 sec^{-1}, then M26A1E1 propellant will also be less likely to exhibit as significant an increase in apparent burning rate as M14 propellant. In addition, previous work has shown that propellant vulnerability is correlated to fracture damage (cold propellant is more vulnerable and mechanically friable than hot propellant).

7. REFERENCES

Furrier, P. Telephone conversation. Hercules, Inc., Kenvil, N.J., June, 1992.

Gazonas, G.A., A. Juhasz and J.C. Ford "Strain Rate Insensitivity of Damage-Induced Surface Area in M30 and JA2 Gun Propellants." BRL-TR-3251, U.S. Army Ballistic Research Laboratory, Aberdeen Proving Ground, Maryland, August, 1991.

Gazonas, G.A. and J.C. Ford "Uniaxial Compression Testing of M30 and JA2 Gun Propellants Using a Statistical Design Strategy." Experimental Mechanics, Vol. 32, pp. 154-162, 1992.

Gazonas, G.A., "The Mechanical Response of M30, XM39, and JA2 Propellants at Strain Rates from 10^{-2} to 250 sec^{-1}." BRL-TR-3181, U.S. Army Ballistic Research Laboratory, Aberdeen Proving Ground, Maryland, January, 1991.

Lu, P., B. Strauss, S. Moy and R.J. Lieb "Shaped Charge Jet Impact on Gun Propellants - Temperature and Mechanical Properties Effects." 1991 Propulsion Systems Hazards Subcommittee Meeting, March 1991.

Malvern, L.E. Introduction to the Mechanics of a Continuous Medium. Prentice-Hall, Inc., Englewood Cliffs, New Jersey, 1969.

No. of Copies	Organization
2	Administrator Defense Technical Info Center ATTN: DTIC-DDA Cameron Station Alexandria, VA 22304-6145
1	Commander U.S. Army Materiel Command ATTN: AMCAM 5001 Eisenhower Ave. Alexandria, VA 22333-0001
1	Director U.S. Army Research Laboratory ATTN: AMSRL-D 2800 Powder Mill Rd. Adelphi, MD 20783-1145
1	Director U.S. Army Research Laboratory ATTN: AMSRL-OP-CI-AD, Tech Publishing 2800 Powder Mill Rd. Adelphi, MD 20783-1145
2	Commander U.S. Army Armament Research, Development, and Engineering Center ATTN: SMCAR-IMI-I Picatinny Arsenal, NJ 07806-5000
2	Commander U.S. Army Armament Research, Development, and Engineering Center ATTN: SMCAR-TDC Picatinny Arsenal, NJ 07806-5000
1	Director Benet Weapons Laboratory U.S. Army Armament Research, Development, and Engineering Center ATTN: SMCAR-CCB-TL Watervliet, NY 12189-4050
(Unclass. only)1	Commander U.S. Army Rock Island Arsenal ATTN: SMCRI-IMC-RT/Technical Library Rock Island, IL 61299-5000
1	Director U.S. Army Aviation Research and Technology Activity ATTN: SAVRT-R (Library) M/S 219-3 Ames Research Center Moffett Field, CA 94035-1000

No. of Copies	Organization
1	Commander U.S. Army Missile Command ATTN: AMSMI-RD-CS-R (DOC) Redstone Arsenal, AL 35898-5010
1	Commander U.S. Army Tank-Automotive Command ATTN: ASQNC-TAC-DIT (Technical Information Center) Warren, MI 48397-5000
1	Director U.S. Army TRADOC Analysis Command ATTN: ATRC-WSR White Sands Missile Range, NM 88002-5502
1	Commandant U.S. Army Field Artillery School ATTN: ATSF-CSI Ft. Sill, OK 73503-5000
(Class. only)1	Commandant U.S. Army Infantry School ATTN: ATSH-CD (Security Mgr.) Fort Benning, GA 31905-5660
(Unclass. only)1	Commandant U.S. Army Infantry School ATTN: ATSH-CD-CSO-OR Fort Benning, GA 31905-5660
1	WL/MNOI Eglin AFB, FL 32542-5000
	Aberdeen Proving Ground
2	Dir, USAMSAA ATTN: AMXSY-D AMXSY-MP, H. Cohen
1	Cdr, USATECOM ATTN: AMSTE-TC
1	Dir, ERDEC ATTN: SCBRD-RT
1	Cdr, CBDA ATTN: AMSCB-CI
1	Dir, USARL ATTN: AMSRL-SL-I
10	Dir, USARL ATTN: AMSRL-OP-CI-B (Tech Lib)

No. of Copies	Organization
1	Chairman DOD Explosives Safety Board Room 856-C Hoffman Bldg. 1 2461 Eisenhower Avenue Alexandria, VA 22331-0600
1	Headquarters U.S. Army Materiel Command ATTN: AMCICP-AD, M. Fisette 5001 Eisenhower Ave. Alexandria, VA 22333-0001
1	U.S. Army Ballistic Missile Defense Systems Command Advanced Technology Center P.O. Box 1500 Huntsville, AL 35807-3801
1	Department of the Army Office of the Product Manager 155mm Howitzer, M109A6, Paladin ATTN: SFAE-AR-HIP-IP, Mr. R. De Kleine Picatinny Arsenal, NJ 07806-5000
3	Project Manager Advanced Field Artillery System ATTN: SFAE-ASM-AF-E LTC D. Ellis T. Kuriata J. Shields Picatinny Arsenal, NJ 07801-5000
1	Project Manager Advanced Field Artillery System ATTN: SFAE-ASM-AF-Q, W. Warren Picatinny Arsenal, NJ 07801-5000
2	Commander Production Base Modernization Agency U.S. Army Armament Research, Development, and Engineering Center ATTN: AMSMC-PBM. A. Siklosi AMSMC-PBM-E, L. Laibson Picatinny Arsenal, NJ 07806-5000
4	PEO-Armaments Project Manager Tank Main Armament System ATTN: AMCPM-TMA AMCPM-TMA-105 AMCPM-TMA-120 AMCPM-TMA-AS, H. Yuen Picatinny Arsenal, NJ 07806-5000
5	Commander U.S. Army Armament Research, Development, and Engineering Center ATTN: SMCAR-CCD, D. Spring SMCAR-CCH-V, C. Mandala E. Fennell SMCAR-CCH-T, L. Rosendorf SMCAR-CCS Picatinny Arsenal, NJ 07806-5000
19	Commander U.S. Army Armament Research, Development, and Engineering Center ATTN: SMCAR-AEE, J. Lannon SMCAR-AEE-B, A. Beardell D. Downs S. Einstein S. Westley S. Bernstein J. Rutkowski B. Brodman P. O'Reilly R. Cirincione A. Grabowsky P. Hui J. O'Reilly SMCAR-AEE-WW, M. Mezger J. Pinto D. Wiegand P. Lu C. Hu SMCAR-AES, S. Kaplowitz Picatinny Arsenal, NJ 07806-5000
1	Commander U.S. Army Armament Research, Development and Engineering Center ATTN: SMCAR-HFM, E. Barrieres Picatinny Arsenal, NJ 07806-5000

No. of Copies	Organization
9	Commander U.S. Army Armament Research, Development and Engineering Center ATTN: SMCAR-FSA-T, M. Salsbury SMCAR-FSA-F, LTC R. Riddle SMCAR-FSC, G. Ferdinand SMCAR-FS, T. Gora SMCAR-FS-DH, J. Feneck SMCAR-FSS-A, R. Kopman B. Machek L. Pinder SMCAR-FSN-N, K. Chung Picatinny Arsenal, NJ 07806-5000
3	Director Benet Weapons Laboratories ATTN: SMCAR-CCB-RA, G.P. O'Hara G.A. Pflegl SMCAR-CCB-S, F. Heiser Watervliet, NY 12189-4050
2	Commander U.S. Army Research Office ATTN: Technical Library D. Mann P.O. Box 12211 Research Triangle Park, NC 27709-2211
1	Commander, USACECOM R&D Technical Library ATTN: ASQNC-ELC-IS-L-R, Myer Center Fort Monmouth, NJ 07703-5301
1	Commander U.S. Army Harry Diamond Laboratory ATTN: SLCHD-TA-L 2800 Powder Mill Rd. Adelphi, MD 20783-1145
1	Commandant U.S. Army Aviation School ATTN: Aviation Agency Fort Rucker, AL 36360
1	Program Manager U.S. Tank-Automotive Command ATTN: AMCPM-ABMS, T. Dean Warren, MI 48092-2498

No. of Copies	Organization
1	Project Manager U.S. Tank-Automotive Command Fighting Vehicle Systems ATTN: SFAE-ASM-BV Warren, MI 48397-5000
1	Project Manager, Abrams Tank System ATTN: SFAE-ASM-AB Warren, MI 48397-5000
1	Director HQ, TRAC RPD ATTN: ATCD-MA Fort Monroe, VA 23651-5143
2	Director U.S. Army Materials Technology Laboratory ATTN: SLCMT-ATL (2 cps) Watertown, MA 02172-0001
1	Commander U.S. Army Belvoir Research and Development Center ATTN: STRBE-WC Fort Belvoir, VA 22060-5006
1	Director U.S. Army TRAC-Ft. Lee ATTN: ATRC-L, Mr. Cameron Fort Lee, VA 23801-6140
1	Commandant U.S. Army Command and General Staff College Fort Leavenworth, KS 66027
1	Commandant U.S. Army Special Warfare School ATTN: Rev and Trng Lit Div Fort Bragg, NC 28307
1	Commander Radford Army Ammunition Plant ATTN: SMCAR-QA/HI LIB Radford, VA 24141-0298

No. of Copies	Organization
1	Commander U.S. Army Foreign Science and Technology Center ATTN: AMXST-MC-3 220 Seventh Street, NE Charlottesville, VA 22901-5396
2	Commandant U.S. Army Field Artillery Center and School ATTN: ATSF-CO-MW, E. Dublisky ATSF-CN, P. Gross Ft. Sill, OK 73503-5600
1	Commandant U.S. Army Armor School ATTN: ATZK-CD-MS, M. Falkovitch Armor Agency Fort Knox, KY 40121-5215
2	Commander Naval Sea Systems Command ATTN: SEA 62R SEA 64 Washington, DC 20362-5101
1	Commander Naval Air Systems Command ATTN: AIR-954-Tech Library Washington, DC 20360
4	Commander Naval Research Laboratory ATTN: Technical Library Code 4410, K. Kailasanate J. Boris E. Oran Washington, DC 20375-5000
1	Office of Naval Research ATTN: Code 473, R.S. Miller 800 N. Quincy Street Arlington, VA 22217-9999
1	Office of Naval Technology ATTN: ONT-213, D. Siegel 800 N. Quincy St. Arlington, VA 22217-5000

No. of Copies	Organization
4	Commander Naval Surface Warfare Center ATTN: Code 730 Code R-[illegible], R. Bernecker H. Sandusky Silver Spring, MD 20903-5000
7	Commander Naval Surface Warfare Center ATTN: T.C. Smith K. Rice S. Mitchell S. Peters J. Consaga C. Gotzmer Technical Library Indian Head, MD 20640-5000
5	Commander Naval Surface Warfare Center ATTN: Code G30, Code G32, Code G33, J.L. East T. Doran Code E23 Technical Library Dahlgren, VA 22448-5000
5	Commander Naval Air Warfare Center ATTN: Code 388, C.F. Price T. Boggs Code 3895, T. Parr R. Derr Information Science Division China Lake, CA 93555-6001
2	Commanding Officer Naval Underwater Systems Center ATTN: Code 5B331, R.S. Lazar Technical Library Newport, RI 02840
1	AFOSR/NA ATTN: J. Tishkoff Bolling AFB, D.C. 20332-6448
1	OLAC PL/TSTL ATTN: D. Shiplett Edwards AFB, CA 93523-5000

No. of Copies	Organization
3	AL/LSCF ATTN: J. Levine L. Quinn T. Edwards Edwards AFB, CA 93523-5000
1	WL/MNAA ATTN: B. Simpson Eglin AFB, FL 32542-5434
1	WL/MNME Energetic Materials Branch 2306 Perimeter Rd. STE 9 Eglin AFB, FL 32542-5910
1	WL/MNSH ATTN: R. Drabczuk Eglin AFB, FL 32542-5434
2	NASA Langley Research Center ATTN: M.S. 408, W. Scallion D. Witcofski Hampton, VA 23605
1	Central Intelligence Agency Office of the Central References Dissemination Branch Room GE-47, HQS Washington, DC 20502
1	Central Intelligence Agency ATTN: J. Backofen NHB, Room 5N01 Washington, DC 20505
1	SDIO/TNI ATTN: L.H. Caveny Pentagon Washington, DC 20301-7100
1	SDIO/DA ATTN: E. Gerry Pentagon Washington, DC 21301-7100
2	HQ DNA ATTN: D. Lewis A. Fahey 6801 Telegraph Rd. Alexandria, VA 22310-3398

No. of Copies	Organization
1	Director Sandia National Laboratories Energetic Materials & Fluid Mechanics Department, 1512 ATTN: M. Baer P.O. Box 5800 Albuquerque, NM 87185
1	Director Sandia National Laboratories Combustion Research Facility ATTN: R. Carling Livermore, CA 94551-0469
4	Director Lawrence Livermore National Laboratory ATTN: L-355, A. Buckingham G. Benedetti M. Finger L-324, M. Constantino P.O. Box 808 Livermore, CA 94550-0622
2	Director Los Alamos Scientific Lab ATTN: T3/D. Butler M. Division/B. Craig P.O. Box 1663 Los Alamos, NM 87544
3	Battelle Columbus Laboratories ATTN: TACTEC Library, J.N. Huggins V. Levin 505 King Avenue Columbus, OH 43201-2693
1	Battelle PNL ATTN: Mr. Mark Garnich P.O. Box 999 Richland, WA 99352
1	Institute of Gas Technology ATTN: D. Gidaspow 3424 S. State Street Chicago, IL 60616-3896

No. of Copies	Organization
1	Institute for Advanced Technology ATTN: T.M. Krehne The University of Texas of Austin 4030-2 W. Braker Lane Austin, TX 78759-5329
2	CPIA - JHU ATTN: Hary J. Hoffman T. Christian 10630 Little Patuxent Parkway Suite 202 Columbia, MD 21044-3200
1	Brigham Young University Department of Chemical Engineering ATTN: M. Beckstead Provo, UT 84601
1	Jet Propulsion Laboratory California Institute of Technology ATTN: L.D. Strand, MS 125/224 4800 Oak Grove Drive Pasadena, CA 91109
1	California Institute of Technology 204 Karman Lab Main Stop 301-46 ATTN: F.E.C. Culick 1201 E. California Street Pasadena, CA 91109
3	Georgia Institute of Technology School of Aerospace Engineering ATTN: B.T. Zim E. Price W.C. Strahle Atlanta, GA 30332
1	Massachusetts Institute of Technology Department of Mechanical Engineering ATTN: T. Toong 77 Massachusetts Avenue Cambridge, MA 02139-4307
1	University of Illinois Department of Mechanical/Industry Engineering ATTN: H. Krier 144 MEB; 1206 N. Green St. Urbana, IL 61801-2978

No. of Copies	Organization
1	University of Maryland ATTN: Dr. J.D. Anderson College Park, MD 20740
1	University of Massachusetts Department of Mechanical Engineering ATTN: K. Jakus Amherst, MA 01002-0014
1	University of Minnesota Department of Mechanical Engineering ATTN: E. Fletcher Minneapolis, MN 55414-3368
3	Pennsylvania State University Department of Mechanical Engineering ATTN: V. Yang K. Kuo C. Merkle University Park, PA 16802-7501
1	Rensselaer Polytechnic Institute Department of Mathematics Troy, NY 12181
1	Stevens Institute of Technology Davidson Laboratory ATTN: R. McAlevy III Castle Point Station Hoboken, NJ 07030-5907
1	Rutgers University Department of Mechanical and Aerospace Engineering ATTN: S. Temkin University Heights Campus New Brunswick, NJ 08903
1	University of Southern California Mechanical Engineering Department ATTN: 0HE200, M. Gerstein Los Angeles, CA 90089-5199
1	University of Utah Department of Chemical Engineering ATTN: A. Baer Salt Lake City, UT 84112-1194
1	Washington State University Department of Mechanical Engineering ATTN: C.T. Crowe Pullman, WA 99163-5201

No. of Copies	Organization
1	AFELM, The Rand Corporation ATTN: Library D 1700 Main Street Santa Monica, CA 90401-3297
1	Arrow Technology Associates, Inc. ATTN: W. Hathaway P.O. Box 4218 South Burlington, VT 05401-0042
3	AAI Corporation ATTN: J. Hebert J. Frankle D. Cleveland P.O. Box 126 Hunt Valley, MD 21030-0126
2	Alliant Techsystems, Inc. ATTN: R.E. Tompkins J. Kennedy 7225 Northland Dr. Brooklyn Park, MN 55428
1	AVCO Everett Research Laboratory ATTN: D. Stickler 2385 Revere Beach Parkway Everett, MA 02149-5936
1	General Applied Sciences Lab ATTN: J. Erdos 77 Raynor Ave. Ronkonkama, NY 11779-6649
1	General Electric Company Tactical System Department ATTN: J. Mandzy 100 Plastics Ave. Pittsfield, MA 01201-3698
1	IITRI ATTN: M.J. Klein 10 W. 35th Street Chicago, IL 60616-3799
5	Hercules, Inc. Radford Army Ammunition Plant ATTN: D.A. Worrell W.J. Worrell R. Goft C. Chandler L. Rivenbark Radford, VA 24141-0299

No. of Copies	Organization
2	Hercules, Inc. Allegheny Ballistics Laboratory ATTN: William B. Walkup Thomas F. Farabaugh P.O. Box 210 Rocket Center, WV 26726
1	Hercules, Inc. Hercules Plaza ATTN: B.M. Riggleman Wilmington, DE 19894
1	MBR Research Inc. ATTN: Dr. Moshe Ben-Reuven 601 Ewing St., Suite C-22 Princeton, NJ 08540
1	Olin Corporation Badger Army Ammunition Plant ATTN: F.E. Wolf Baraboo, WI 53913
3	Olin Ordnance ATTN: E.J. Kirschke A.F. Gonzalez D.W. Worthington P.O. Box 222 St. Marks, FL 32355-0222
1	Olin Ordnance ATTN: H.A. McElroy 10101 9th Street, North St. Petersburg, FL 33716
1	Paul Gough Associates, Inc. ATTN: P.S. Gough 1048 South St. Portsmouth, NH 03801-5423
1	Physics International Library ATTN: H. Wayne Wampler P.O. Box 5010 San Leandro, CA 94577-0599
2	Princeton Combustion Research Laboratories, Inc. ATTN: N. Mer N.A. Messina Princeton Corporate Plaza 11 Deerpark Dr., Bldg IV, Suite 119 Monmouth Junction, NJ 08852

No. of Copies	Organization
3	Rockwell International Rocketdyne Division ATTN: BA08, J. Flanagan J. Gray R.B. Edelman 6633 Canoga Avenue Canoga Park, CA 91303-2703
2	Rockwell International Science Center ATTN: Dr. S. Chakravarthy Dr. S. Palaniswamy 1049 Camino Dos Rios P.O. Box 1085 Thousand Oaks, CA 91360
1	Southwest Research Institute ATTN: J.P. Riegel 6220 Culebra Road P.O. Drawer 28510 San Antonio, TX 78228-0510
1	Sverdrup Technology, Inc. ATTN: Dr. John Deur 2001 Aerospace Parkway Brook Park, OH 44142
2	Thiokol Corporation Elkton Division ATTN: R. Biddle Tech Library P.O. Box 241 Elkton, MD 21921-0241
1	Veritay Technology, Inc. ATTN: E. Fisher 4845 Millersport Hwy. East Amherst, NY 14501-0305
1	Universal Propulsion Company ATTN: H.J. McSpadden 25401 North Central Ave. Phoenix, AZ 85027-7837
1	SRI International Propulsion Sciences Division ATTN: Tech Library 333 Ravenwood Avenue Menlo Park, CA 94025-3493

No. of Copies	Organization
	Aberdeen Proving Ground
1	Cdr, USACSTA ATTN: STECS-PO/R. Hendricksen

No. of Copies	Organization
1	Ernst-Mach-Institut ATTN: Dr. R. Heiser Haupstrasse 18 Weil am Rheim Germany
1	Defence Research Agency, Military Division ATTN: C. Woodley RARDE Fort Halstead Sevenoaks, Kent, TN14 7BP England
1	School of Mechanical, Materials, and Civil Engineering ATTN: Dr. Bryan Lawton Royal Military College of Science Shrivenham, Swindon, Wiltshire, SN6 8LA England
2	Institut Saint Louis ATTN: Dr. Marc Giraud Dr. Gunther Sheets Postfach 1260 7858 Weail am Rhein 1 Germany

No. of Copies	Organization
1	Explosive Ordnance Division ATTN: A. Wildegger-Gaissmaier Defence Science and Technology Organisation P.O. Box 1750 Salisbury, South Australia 5108
1	Armaments Division ATTN: Dr. J. Lavigne Defence Research Establishment Valcartier 2459, Pie XI Blvd., North P.O. Box 8800 Courcelette, Quebec G0A 1R0 Canada
1	U.S. Army European Research Office ATTN: Dr. Roy E. Richenbach Box 65 FPO New York 09510-1500

INTENTIONALLY LEFT BLANK.

USER EVALUATION SHEET/CHANGE OF ADDRESS

This Laboratory undertakes a continuing effort to improve the quality of the reports it publishes. Your comments/answers to the items/questions below will aid us in our efforts.

1. ARL Report Number ARL-TR-79 Date of Report February 1993

2. Date Report Received ____________________

3. Does this report satisfy a need? (Comment on purpose, related project, or other area of interest for which the report will be used.) ____________________

4. Specifically, how is the report being used? (Information source, design data, procedure, source of ideas, etc.) ____________________

5. Has the information in this report led to any quantitative savings as far as man-hours or dollars saved, operating costs avoided, or efficiencies achieved, etc? If so, please elaborate. ____________________

6. General Comments. What do you think should be changed to improve future reports? (Indicate changes to organization, technical content, format, etc.) ____________________

CURRENT ADDRESS

Organization

Name

Street or P.O. Box No.

City, State, Zip Code

7. If indicating a Change of Address or Address Correction, please provide the Current or Correct address above and the Old or Incorrect address below.

OLD ADDRESS

Organization

Name

Street or P.O. Box No.

City, State, Zip Code

(Remove this sheet, fold as indicated, staple or tape closed, and mail.)

DEPARTMENT OF THE ARMY

OFFICIAL BUSINESS

BUSINESS REPLY MAIL
FIRST CLASS PERMIT No 0001, APG, MD

Postage will be paid by addressee

NO POSTAGE
NECESSARY
IF MAILED
IN THE
UNITED STATES

Director
U.S. Army Research Laboratory
ATTN: AMSRL-OP-CI-B (Tech Lib)
Aberdeen Proving Ground, MD 21005-5066

END

FILMED

DATE: 4-93

DTIC